

# Replacing Automatic Differentiation by Sobolev Cubatures fastens Physics Informed Neural Nets and strengthens their Approximation Power

Juan Esteban Suarez Cardona<sup>1</sup> Michael Hecht<sup>1</sup>

## Abstract

We present a novel class of approximations for variational losses, being applicable for the training of physics-informed neural nets (PINNs). The loss formulation reflects classic Sobolev space theory for partial differential equations and their weak formulations. The loss computation rests on an extension of *Gauss-Legendre cubatures*, we term *Sobolev cubatures*, replacing *automatic differentiation (A.D.)*. We prove the runtime complexity of training the resulting Sobolev-PINNs (SC-PINNs) to be less than required by PINNs relying on A.D. On top of one-to-two order of magnitude speed-up the SC-PINNs are demonstrated to achieve closer solution approximations for prominent forward and inverse PDE problems than established PINNs achieve.

## 1. Introduction

Partial differential equations (PDEs) are omnipresent mathematical models governing the dynamics and (physical) laws of complex systems (Jost, 2002; Brezis, 2011). However, analytic PDE solutions are rarely known for most of the systems being the center of current research. Therefore, there is a strong demand on efficient and accurate numerical solvers and simulations.

Machine learning methods such as: Physics-Informed GAN (Arjovsky et al., 2017), Deep Galerkin Method (Sirignano & Spiliopoulos, 2018), and Physics Informed Neural Networks (PINNs) (Raissi et al., 2019), gain big traction in the scientific computing community. In contrast to clas-

sic solvers, PINNs provide a neural net (NN) surrogate model parametrizing the solution space of the PDEs. PINN-learning is given by minimizing a variational problem, which is typically formulated in  $L^2$ -loss terms

$$\int_{\Omega} \|\hat{u}(x) - u(x)\|^2 d\Omega \approx \frac{1}{|P|} \sum_{p \in P} \|\hat{u}(p) - u(p)\|^2 \quad (1)$$

being approximated by mean square errors (MSE) in random nodes  $P$ , (Yang et al., 2020), (Long et al., 2018).

However, due to the complexity of the underlying non-linear, non-convex variational problem, theoretical and computational challenges arise when demanding to guarantee convergence to PDE solutions of high accuracy.

### 1.1. Related Work

The importance of the present computational challenge is manifest in the large number of previous works. Consequently, an exhaustive overview of the literature cannot be given here. Instead, we restrict ourselves to mentioning those contributions that directly relate to or inspired our work.

#### 1.1.1. CLASSIC NUMERICAL METHODS

Main classic numerical solvers divide into: Finite Elements (Ern & Guermond, 2004); Finite Differences (LeVeque, 2007); Finite Volumes (Bernardi & Maday, 1997); Spectral Methods (Bernardi & Maday, 1997) and Particle Methods (Li & Liu, 2007). These class of methods provide solutions with high accuracy, but come with the cost of having limited flexibility with respect to the type of problems they can solve. This includes especially inverse problems, as PDE parameter inference, being a hard challenge for the aforementioned methods. In contrast, the variational formulation defining the PINN training provides the desired flexibility, but comes again with the cost of less reachable accuracy.

We focus on two recent approaches addressing the stability and accuracy of PINNs.

#### 1.1.2. VARIATIONAL PINNs (VPINNs)

VPINNs were introduced in (Kharazmi et al., 2019), (Kharazmi et al., 2020) formulating variational Sobolev

<sup>1</sup>CASUS - Center for Advanced System Understanding, Helmholtz-Zentrum Dresden-Rossendorf e.V. (HZDR), Görlitz, Germany. Correspondence to: Juan Esteban Suarez Cardona <j.suarez-cardona@hzdr.de>, Michael Hecht <m.hecht@hzdr.de>.

This work was partially funded by the Center of Advanced Systems Understanding (CASUS), financed by Germany's Federal Ministry of Education and Research (BMBF) and by the Saxon Ministry for Science, Culture and Tourism (SMWK) with tax funds on the basis of the budget approved by the Saxon State Parliament.

losses for PINN-training. The approach relies on exploiting analytic integration and differentiation formulas of shallow neural networks with specified activation functions. The method is extended by using quadratures and automatic differentiation for computing the losses and complemented by a domain decomposition approach.

### 1.1.3. INVERSE DIRICHLET LOSS BALANCING

With the Inverse Dirichlet method (Maddu et al., 2021) the numerical stability of PINNS was increased by dynamically balancing the occurring gradient amplitudes, which if unbalanced cause numerical stiffness phenomena (Wang et al., 2021). The PINN formulation, however, rests on classic MSE losses.

## 1.2. Contribution

We provide the notion of Sobolev cubatures providing close approximations of the corresponding Sobolev norms, extending the  $L^2$ -integrals in Eq (1). While classic weak PDE formulations rest on the Sobolev spaces, our approach enables to mathematically prove the resulting PINNs to converge to strong solutions of sufficiently regular posed PDE problems. Moreover, the Sobolev cubatures enable to replace *automatic differentiation* (A.D.) (Baydin et al., 2018b) by *polynomial differentiation* (P.D.). Being mostly the bottleneck, for both, runtime and accuracy performance, replacing A.D. by P.D. does not only result in more efficient PINNs, but allows to reach much closer solution approximations (several magnitudes), as demonstrated herein.

## 2. Sobolev Cubatures

Closer approximations of  $L^2$ -integrals than reachable by prominent MSE approaches can be derived by applying classic *Gauss-Legendre cubatures* (see e.g. Stroud, 1971; 2011; Trefethen, 2017a;b; 2019) or even further extension to what we call *Sobolev cubatures*, presented herein. The notions of this section follow classic concepts of spectral methods (Canuto et al., 2007; Trefethen, 2019). We start by introducing fixing the notation used in the article.

### 2.1. Notation

We consider neural nets (NNs)  $\hat{u}_\theta(\cdot)$  with  $m_1, m_2$ -dimensional input/output domain  $m_1, m_2 \in \mathbb{N}$  of fixed architecture  $\Xi_{m_1, m_2}$  (specifying number and depth of the hidden layers, with continuous piecewise smooth activation functions  $\sigma(x)$ , e.g. ReLU or ELU. Further,  $\Upsilon_{\Xi_{m_1, m_2}}$  denotes the parameter space of the weights (and bias)  $\theta = (v, b) \in W = V \times B \subseteq \mathbb{R}^K$ ,  $K \in \mathbb{N}$ , see e.g. (Anthony & Bartlett, 2009; Goodfellow et al., 2016).

Throughout this article we denote with  $\Omega = [-1, 1]^m$

the  $m$ -dimensional *standard hypercube* and with  $\|x\|_p = (\sum_{i=1}^m |x_i|^p)^{1/p}$ ,  $x = (x_1, \dots, x_m) \in \mathbb{R}^m$ ,  $1 \leq p < \infty$ ,  $\|x\|_\infty = \max_{1 \leq i \leq m} |x_i|$  the  $l_p$ -norm. We recommend (Adams & Fournier, 2003; Brezis, 2011) for an excellent overview on functional analysis and the Sobolev spaces

$$H^k(\Omega, \mathbb{R}) = \{f \in L^2(\Omega, \mathbb{R}) : D^\alpha f \in L^2(\Omega, \mathbb{R})\}, k \in \mathbb{N}$$

given by all  $L^2$ -integrable functions  $f : \Omega \rightarrow \mathbb{R}$  with existing  $L^2$ -integrable weak derivatives  $D^\alpha f = \partial_{x_1}^{\alpha_1} \dots \partial_{x_m}^{\alpha_m} f$  up to order  $k$ . In fact,  $H^k(\Omega, \mathbb{R})$  is a Hilbert space with inner product

$$\langle f, g \rangle_{H^k(\Omega)} = \sum_{0 \leq |\alpha| \leq k} \langle D^\alpha f, D^\alpha g \rangle_{L^2(\Omega)}$$

and norm  $\|f\|_{H^k(\Omega)}^2 = \langle f, f \rangle_{H^k(\Omega)}$ , where  $H^0(\Omega, \mathbb{R}) = L^2(\Omega, \mathbb{R})$ , with  $\langle f, g \rangle_{L^2(\Omega)} = \int_\Omega f \cdot g \, d\Omega$ .

From the *Trace Theorem* (Adams & Fournier, 2003), we find furthermore that whenever  $H \subseteq \mathbb{R}^m$  is a hyperplane of co-dimension 1, then the induced restriction

$$\varrho : H^k(\Omega, \mathbb{R}) \rightarrow H^{k-1/2}(\Omega \cap H, \mathbb{R}) \quad (2)$$

is continuous, i.e.,  $\|f|_{\Omega \cap H}\|_{H^{k-1/2}(\Omega \cap H)} \leq d \|f\|_{H^k(\Omega)}$  for some  $d = d(m, \Omega) \in \mathbb{R}^+$ .

Further,  $C^k(\Omega, \mathbb{R})$ ,  $k \in \mathbb{N} \cup \{\infty\}$  denote the *Banach spaces* of  $k$ -times continuously differentiable functions with norm  $\|f\|_{C^k(\Omega)} = \sum_{i=0}^k \sup_{x \in \Omega, \|\alpha\|_1=i} |D^\alpha f(x)|$ .

$\Pi_{m,n} = \text{span}\{x^\alpha\}_{\|\alpha\|_\infty \leq n}$  denotes the  $\mathbb{R}$ -vector space of all real polynomials in  $m$  variables spanned by all monomials  $x^\alpha = \prod_{i=1}^m x_i^{\alpha_i}$  of maximum degree  $n \in \mathbb{N}$  and  $A_{m,n} = \{\alpha \in \mathbb{N}^m : \|\alpha\|_\infty \leq n\}$  the corresponding multi-index set with  $|A_{m,n}| = (n+1)^m$ . We order  $A_{m,n}$  with respect to the *lexicographic order*  $\preceq$ . Let  $D = (d_{i,j})_{1 \leq i, j \leq |A_{m,n}|} \in \mathbb{R}^{|A_{m,n}| \times |A_{m,n}|}$  be a matrix. We slightly abuse notation by writing

$$D = (d_{\alpha, \beta})_{\alpha, \beta \in A_{m,n}}, \quad (3)$$

with  $d_{\alpha, \beta}$  being the  $\alpha$ -th,  $\beta$ -th entry of  $D$ .

### 2.2. Orthogonal Polynomials

Let  $m, n \in \mathbb{N}$  we consider the  $m$ -dimensional Legendre grids  $P_{m,n} = \oplus_{i=1}^m \text{Leg}_n \subseteq \Omega$ , where  $\text{Leg}_n = \{p_0, \dots, p_n\}$  are the  $n+1$  Legendre nodes given by the roots of the Legendre polynomials of degree  $n+2$  and denote  $p_\alpha = (p_{\alpha_1}, \dots, p_{\alpha_m}) \in P_{m,n}$ . It is a classic fact (Stroud, 1971; 2011; Trefethen, 2017a; 2019) that the Lagrange polynomials  $L_\alpha \in \Pi_{m,n}$ ,  $\alpha \in A_{m,n}$  given by

$$L_\alpha = \prod_{i=1}^m l_{\alpha_i, i}, \quad l_{j,i} = \prod_{h \neq j, h=0}^n \frac{x_i - p_h}{p_j - p_h}, \quad (4)$$

$p_h \in \text{Leg}_n$  satisfy  $L_\alpha(p_\beta) = \delta_{\alpha,\beta}$ ,  $\forall \alpha, \beta \in A_{m,n}$  and yield an orthogonal  $L^2$ -basis of  $\Pi_{m,n}$ , i.e.,

$$\langle L_\alpha, L_\beta \rangle_{L^2(\Omega)} = \int_{\Omega} L_\alpha(x) L_\beta(x) d\Omega = w_\alpha \delta_{\alpha,\beta},$$

$\forall \alpha, \beta \in A_{m,n}$ , where  $\delta_{\cdot,\cdot}$  denotes the Kronecker delta and

$$w_\alpha = \|L_\alpha\|_{L^2(\Omega)}^2 \quad (5)$$

the efficiently computable *Gauss-Legendre cubature weight* (Stroud, 1971; Trefethen, 2019). Consequently, for any polynomial  $Q \in \Pi_{m,2n+1}$  of degree  $2n+1$  the following cubature rule applies:

$$\int_{\Omega} Q(x) d\Omega = \sum_{\alpha \in A_{m,n}} w_\alpha Q(p_\alpha). \quad (6)$$

Summarizing: Polynomials of degree  $2n+1$  can be (numerically) integrated exactly when sampled on the Legendre grid  $P_{m,n}$  of order  $n+1$ . Thanks to  $|P_{m,n}| = (n+1)^m \ll (2n+1)^m$  this makes *Gauss-Legendre integration* a very powerful integration scheme yielding

$$\|Q\|_{L^2(\Omega)}^2 = \int_{\Omega_m} Q(x)^2 d\Omega_m = \sum_{\alpha \in A_{m,n}} Q(p_\alpha)^2 w_\alpha. \quad (7)$$

for all  $Q \in \Pi_{m,n}$ .

### 2.3. Differential Operators on $\Pi_{m,n}$

Based on Eq. (4) we derive exact matrix representations of differential operators on the polynomial spaces  $\Pi_{m,n}$  allowing to extend Eq. (7) to close approximations of the Sobolev norms for general Sobolev functions  $f \in H^k(\Omega, \mathbb{R})$ ,  $k \in \mathbb{N}$ .

For  $L_\alpha \in \Pi_{m,n}$  from Eq. (4) and  $1 \leq i \leq m$  the computation of values  $d_{\alpha,\beta} = \partial_{x_i} L_\alpha(p_\beta)$ ,  $p_\beta \in P_{m,n}$ ,  $\forall \beta \in A_{m,n}$  yields the Lagrange expansion

$$\partial_{x_i} L_\alpha(x) = \sum_{\beta \in A_{m,n}} d_{\alpha,\beta} L_\beta(x). \quad (8)$$

Consequently, the matrix

$$D_i = (d_{\alpha,\beta})_{\alpha,\beta \in A_{m,n}} \in \mathbb{R}^{|A_{m,n}| \times |A_{m,n}|}, \quad (9)$$

represents the finite dimensional truncation of the differential operator  $\partial_{x_i} : C^1(\Omega, \mathbb{R}) \rightarrow C^0(\Omega, \mathbb{R})$  to the polynomial space  $\Pi_{m,n}$  and for  $\beta \in \mathbb{N}^m$  we set

$$D_\beta = \prod_{j=1}^m D_{\beta_j} \quad (10)$$

to be the approximation of  $\partial_\beta := \partial_{x_1}^{\beta_1} \dots \partial_{x_m}^{\beta_m}$ . As a direct consequence of Eq. (7) the following statement applies:

**Theorem 1** (Sobolev cubatures). *Let  $m, n \in \mathbb{N}$ ,  $A_{m,n} \subseteq \mathbb{N}^m$ ,  $P_{m,n} = \{p_\alpha : \alpha \in A_{m,n}\}$ , be the Legendre grid,  $W_{m,n} = \text{diag}(w_\alpha)_{\alpha \in A_{m,n}}$  be the Gauss-Legendre cubature weight matrix, and  $F_{m,n} = (f(p_\alpha))_{\alpha \in A_{m,n}} \in \mathbb{R}^{|A_{m,n}|}$ . Let*

$$W_{m,n,k} = \sum_{\beta \in \mathbb{N}^m, \|\beta\|_1 \leq k} D_\beta^T W_{m,n} D_\beta, \quad (11)$$

with  $D_\beta$  from Eq. (10) be the Sobolev cubature matrix then

$$\|f\|_{H^k(\Omega)}^2 \approx F_{m,n}^T W_{m,n,k} F_{m,n}, \quad (12)$$

is an exact approximation whenever  $f \in \Pi_{m,n}$ .

We conclude that Theorem 1 enables to control the uniform distance  $\|f - g\|_{C^0(\Omega)}$  on the whole domain  $\Omega$ .

**Corollary 2.** *Let the assumptions of Theorem 1 be fulfilled, and  $f, g \in H^k(\Omega, \mathbb{R})$ ,  $k > m/2$  be two Sobolev functions. Assume there is  $n \in \mathbb{N}$  (large enough) such that the residuum  $f - g \in \Pi_{m,n}$  is given by a polynomial with*

$$f(p_\alpha) - g(p_\alpha) = 0, \quad \forall p_\alpha \in P_{m,n}.$$

Then  $f(x) - g(x) = 0$  for all  $x \in \Omega = [-1, 1]^m$ .

*Proof.* Due to Theorem 1 we deduce  $\|f - g\|_{H^k(\Omega)} = 0$ . While the Sobolev Embedding Theorem (Adams & Fournier, 2003) yields the continuous inclusion  $H^k(\Omega, \mathbb{R}) \subseteq C^0(\Omega, \mathbb{R})$ , consequently, we realize that  $\|f - g\|_{C^0(\Omega)} = 0$ , proving the claimed identity.  $\square$

In light of the provided perspectives, we propose the following formalizations of classic PDE problems.

## 3. Strong and weak PDE formulations

We follow (Jost, 2002; Brezis, 2011) to restate classic (weak) PDE formulations and their Sobolev cubature approximations. For the sake of simplicity, we focus on the example of the classic *Poisson equation*.

### 3.1. Poisson equation

For  $f \in C^0(\Omega, \mathbb{R})$  the *strong Poisson problem* with Dirichlet boundary condition  $g \in C^0(\partial\Omega, \mathbb{R})$  seeks for solutions  $u \in C^2(\Omega, \mathbb{R})$  fulfilling:

$$\begin{cases} -\Delta u(x) - f(x) = 0 & , \forall x \in \Omega \\ u(x) - g(x) = 0 & , \forall x \in \partial\Omega. \end{cases} \quad (13)$$

We can weaken the initial regularity assumptions by demanding  $u \in H^2(\Omega, \mathbb{R})$  to satisfy the PDE in the integral sense, yielding the *strong variational formulation*:

$$\begin{cases} \int_{\Omega} (-\Delta u + f) \phi d\Omega = 0 & , \forall \phi \in \Gamma(\Omega, \mathbb{R}) \\ \int_{\partial\Omega} (u - g) \phi dS = 0 & , \forall \phi \in \Gamma(\partial\Omega, \mathbb{R}), \end{cases} \quad (14)$$

where  $\Gamma(\Omega, \mathbb{R}) = \{\phi \in C^\infty(\Omega, \mathbb{R}) : \|\phi\|_{C^0(\Omega)} \leq 1\}$  denotes the space of *test functions*. We can weaken the regularity assumptions even more by imposing  $u \in H^1(\Omega, \mathbb{R})$  to satisfy the following *weak variational formulation*:

$$\begin{cases} \int_{\Omega} (\nabla u \cdot \nabla \phi + f\phi) d\Omega - \int_{\partial\Omega} (\nabla u \phi) \eta dS = 0 \\ \int_{\partial\Omega} (u - g)\phi dS = 0, \end{cases} \quad (15)$$

where we applied integration by parts and  $\eta$  denotes the (piecewise smooth) normal field of  $\partial\Omega$ .

### 3.2. Residual loss in terms of Sobolev cubatures

We translate the introduced PDE formulations into *variational optimization problems* demanded to be minimized by the PINNs framework. In addition to Sobolev cubature matrix  $W_{m,n,k}$  from Eq. (11) the matrices

$$\begin{aligned} U_{m,n,k} &= \sum_{\beta \in \mathbb{N}^m, \|\beta\|_1 \leq k} D_{\beta}^T W_{m,n}^2 D_{\beta}, \\ V_{m-1,n,k-1/2} &= \sum_{\beta \in \mathbb{N}^{m-1}, \|\beta\|_1 \leq k-1/2} D_{\beta}^T W_{m-1,n}^2 D_{\beta}, \end{aligned} \quad (16)$$

relying on Theorem 1, are the key ingredient in this regard.

The **strong residual loss**  $\mathcal{L}_{\text{strong}} : C^2(\Omega, \mathbb{R}) \rightarrow \mathbb{R}$ , relies on the residuals

$$\begin{aligned} \mathcal{L}_{\text{strong}}(u) &= r_{\text{strong},0}(u) + s_{\text{strong},0}(u) \\ &= \|\Delta u + f\|_{L^2(\Omega)}^2 + \|u|_{\partial\Omega} - g\|_{L^2(\partial\Omega)}^2, \end{aligned}$$

which we extend to  $\mathcal{L}_{\text{strong},k}$ ,  $k \geq 1/2$  with

$$\begin{aligned} \mathcal{L}_{\text{strong},k}(u) &= r_{\text{strong},k}(u) + s_{\text{strong},k}(u) \\ &= \|\Delta u + f\|_{H^k(\Omega)}^2 + \|u|_{\partial\Omega} - g\|_{H^{k-1/2}(\partial\Omega)}^2, \end{aligned} \quad (17)$$

where the  $H^{k-1/2}$ -metric of the second residual  $s_{\text{strong},k}$  reflects the *Trace Theorem* (Eq. (2)). We propose to approximate  $\mathcal{L}_{\text{strong},k}(u) \approx r_{\text{strong},n,k}(u) + s_{\text{strong},n,k}(u)$  by the following Sobolev cubatures:

$$r_{\text{strong},n,k}(u) = R_{m,n}^T W_{m,n,k} R_{m,n}, \quad (18)$$

$$s_{\text{strong},n,k}(u) = S_{m-1,n}^T V_{m-1,n,k-1/2} S_{m-1,n}. \quad (19)$$

Thereby,  $V_{m-1,n,k-1/2} = W_{m-1,n}$  for  $0 \leq k < 1/2$ , and

$$R_{m,n} = -D_{(2,\dots,2)}(\hat{u}(p_{\alpha}, w))_{\alpha \in A_{m,n}} - F_{m,n}, \quad (20)$$

where  $F_{m,n} = (f(p_{\alpha}))_{\alpha \in A_{m,n}}$  and  $D_{(2,\dots,2)} = D_1^2 + \dots + D_m^2 \approx \Delta$  denotes the polynomial approximation of the Laplacian accordingly to Eq. (9). Thus,  $R_{m,n} \in \mathbb{R}^{|A_{m,n}|}$  yields an approximation of  $(\Delta u(p_{\alpha}) + f(p_{\alpha}))_{\alpha \in A_{m,n}}$  by replacing *automatic differentiation* (Baydin et al., 2018b) with *polynomial differentiation*.

Moreover, by summing the residual values  $S_{m-1,n}^{\pm j} = (u(p_{\alpha}^{\pm j}, w) - g(p_{\alpha}^{\pm j}))_{\alpha \in A_{m-1,n}}$  over each face  $\partial\Omega_j^{\pm} = \{x \in \Omega : x_j = \pm 1\}$  of  $\Omega$  we denote the boundary residual as

$$S_{m-1,n} = \sum_{j=0}^m S_{m-1,n}^{\pm j} \in \mathbb{R}^{|A_{m-1,n}|}. \quad (21)$$

The **strong variational loss**  $\mathcal{L}_{\text{strong},k}^{\text{var}} : H^{2+k}(\Omega, \mathbb{R}) \rightarrow \mathbb{R}$  is given by  $\mathcal{L}_{\text{strong},k}^{\text{var}}(u) = r_{\text{strong},k}^{\text{var}}(u) + s_{\text{strong},k}^{\text{var}}(u)$  with

$$r_{\text{strong},k}^{\text{var}}(u) := \sup_{\phi \in \Gamma(\Omega, \mathbb{R})} \langle -\Delta u - f, \phi \rangle_{H^k(\Omega)}^2 \quad (22)$$

$$s_{\text{strong},k}^{\text{var}}(u) = \sup_{\phi \in \Gamma(\partial\Omega, \mathbb{R})} \langle u - g, \phi \rangle_{H^{k-1/2}(\partial\Omega)}^2,$$

where the  $H^{k-1/2}$ -metric of the second residual reflects again the *Trace Theorem* (Eq. (2)). Replacing the test functions  $\phi$  with the Lagrange basis  $L_{\alpha} \in \Pi_{m,n}$ ,  $\alpha \in A_{m,n}$  for the Legendre nodes  $p_{\alpha} \in P_{m,n}$  from Eq. (4) yields the Sobolev cubature approximation  $\mathcal{L}_{\text{strong},k}^{\text{var}}(u) \approx \mathcal{L}_{\text{strong},n,k}^{\text{var}}(u)$ :

$$\begin{aligned} r_{\text{strong},n,k}^{\text{var}}(u) &= R_{m,n}^T U_{m,n,k} R_{m,n}, \\ s_{\text{strong},n,k}^{\text{var}}(u) &= S_{m-1,n}^T V_{m-1,n,k-1/2} S_{m-1,n}, \end{aligned}$$

where  $R_{m,n}$ ,  $S_{m-1,n}$  are as in Eq. (20),(21).

The **weak variational loss**  $\mathcal{L}_{\text{weak},k}^{\text{var}} : H^{1+k}(\Omega, \mathbb{R}) \rightarrow \mathbb{R}$  given by  $\mathcal{L}_{\text{weak},k}^{\text{var}} = r_{\text{weak},k}^{\text{var}}(u) + s_{\text{strong},k}^{\text{var}}(u)$  only differs in the first residual  $r_{\text{weak},k}^{\text{var}}(u)$  from  $\mathcal{L}_{\text{strong},k}^{\text{var}}$  by

$$\begin{aligned} r_{\text{weak},k}^{\text{var}}(u) &= \sup_{\phi \in \Gamma(\Omega, \mathbb{R})} \left( \langle \nabla u, \nabla \phi \rangle_{H^k(\Omega)} + \langle f, \phi \rangle_{H^k(\Omega)} \right. \\ &\quad \left. - \langle \nabla u \phi, \eta \rangle_{H^{k-1/2}(\partial\Omega)} \right). \end{aligned}$$

Yielding the approximates  $\mathcal{L}_{\text{weak},k}^{\text{var}}(u) \approx \mathcal{L}_{\text{weak},n,k}^{\text{var}}(u)$  due to:

$$\sup_{\phi \in \Gamma(\Omega, \mathbb{R})} \langle \nabla u, \nabla \phi \rangle_{H^k(\Omega)} \approx H_{m,n}^T U_{m,n,k} H_{m,n}$$

$$\sup_{\phi \in \Gamma(\Omega, \mathbb{R})} \langle f, \phi \rangle_{H^k(\Omega)} \approx F_{m,n}^T U_{m,n,k} F_{m,n}$$

$$\sup_{\phi \in \Gamma(\Omega, \mathbb{R})} \langle \nabla u \phi, \eta \rangle_{H^{k-1/2}(\partial\Omega)} \approx G_{m-1,n}^T V_{m-1,n,k-1/2} G_{m-1,n},$$

where  $H_{m,n} = \sum_{i=1}^m D_i^T D_i(u(p_{\alpha}))_{\alpha \in A_{m,n}}$ ,  $F_{m,n} = (f(p_{\alpha}))_{\alpha \in A_{m,n}}$ ,  $G_{m-1,n} = e_{\alpha}^T \sum_{i=1}^m D_i(u(p_{\alpha}))_{\alpha \in A_{m,n}}$  and  $U_{m,n,k}$ ,  $V_{m-1,n,k-1/2}$  are the Sobolev cubature matrices from Eq. (16).

Summarizing, the given notions allow to extend Corollary 2 in order to state the following result.

**Theorem 3** (Strong solution approximation). *Let  $m \in \mathbb{N}$ ,  $u \in C^2(\Omega, \mathbb{R})$ ,  $u \in H^{l+k}(\Omega, \mathbb{R})$ ,  $k \geq 0$ ,  $l = 1, 2$  be a regular  $m$ -variate (Sobolev) function.*



i) If the losses vanish,  $\mathcal{L}_{\text{strong},k}(u) = 0$ ,  $\mathcal{L}_{\text{strong},k}^{\text{var}}(u) = 0$ , or  $\mathcal{L}_{\text{weak},k}^{\text{var}}(u) = 0$  then  $u$  is a strong solution of the Poisson equation, respectively, i.e.  $u \in C^2(\Omega, \mathbb{R})$  and solves the strong Poisson problem.

ii) Denoting with  $\mathcal{L}_{\text{strong},n,k}$ ,  $\mathcal{L}_{\text{strong},n,k}^{\text{var}}$ ,  $\mathcal{L}_{\text{weak},n,k}^{\text{var}}$  the loss approximations of degree  $n \in \mathbb{N}$  as given above. Then for all  $\varepsilon > 0$  there is  $n = n(\varepsilon)$  and  $u' \in \Pi_{m,n}$  with  $\|u - u'\|_{C^2(\Omega)} < \varepsilon$ ,  $\|u - u'\|_{H^{l+k}(\Omega)} < \varepsilon$  such that  $\mathcal{L}_{\text{strong},n}(u') = \mathcal{L}_{\text{strong}}(u')$ ,  $\mathcal{L}_{\text{strong},n,k}^{\text{var}}(u') = \mathcal{L}_{\text{strong},k}^{\text{var}}(u')$ ,  $\mathcal{L}_{\text{weak},n,k}^{\text{var}}(u') = \mathcal{L}_{\text{weak},k}^{\text{var}}(u')$ .

*Proof.* Statement i) reflects classic PDE theory (Jost, 2002; Brezis, 2011). ii) follows from  $H^{l+k}(\Omega, \mathbb{R}) \subseteq C^2(\Omega, \mathbb{R})$  and the Stone-Weierstrass theorem (Weierstrass, 1885; De Branges, 1959), stating that any continuous function  $f \in C^0(\Omega, \mathbb{R}) \supseteq C^2(\Omega, \mathbb{R})$  can be uniformly approximated by polynomials. By a bootstrapping argument that implies that polynomials are dense in all  $C^r(\Omega, \mathbb{R})$ ,  $r \in \mathbb{N} \cup \{\infty\}$  with respect to the corresponding norms  $\|\cdot\|_{C^r(\Omega)}$ . While  $C^\infty(\Omega, \mathbb{R}) \subseteq H^{l+k}(\Omega, \mathbb{R})$  is dense (Adams & Fournier, 2003), polynomial approximations  $\|u - u'\|_{H^{l+k}(\Omega)} < \varepsilon$  exist. Due to Theorem 1 the Sobolev cubature losses  $\mathcal{L}_{\text{strong},n}(u')$ ,  $\mathcal{L}_{\text{strong},n,k}^{\text{var}}(u')$ ,  $\mathcal{L}_{\text{weak},n,k}^{\text{var}}(u')$  are exact for  $u' \in \Pi_{m,n}$  proving the statement.  $\square$

We conclude, that apart from the weaker regularity assumptions on the solution  $u : \Omega \rightarrow \mathbb{R}$  required by the variational losses, Theorem 3 theoretically guarantees approximations of strong solutions whenever minimization (by PINN training) reaches  $\mathcal{L}_{\text{strong},n,k}(u')$ ,  $\mathcal{L}_{\text{strong},n,k}^{\text{var}}(u')$ ,  $\mathcal{L}_{\text{weak},n,k}^{\text{var}}(u') \approx 0$  sufficient small losses for  $n \in \mathbb{N}$  large enough.

## 4. Gradient Flow of PINN Training

For a given PINN  $u = \hat{u}(\cdot, w) \in \Xi_{m,1}$ , of fixed architecture, (optimally) adjusted weights  $w \in \Upsilon_{\Xi_{2,1}}$  are demanded, minimizing the loss. NN training is realized as a gradient descent, given by solving the *gradient flow ODE*

$$\begin{aligned} \partial_t w &= -\delta_w \mathcal{L}(\hat{u}(\cdot, w(t))) w_0, \\ &= -\nabla \mathcal{L}(\hat{u}(\cdot, w(t))) \cdot \delta_w \hat{u}(\cdot, w(t)) w_0, \quad w(0) = w_0, \end{aligned} \quad (23)$$

where  $w_0$  is given by the NN initialization and  $\delta_w$  denotes the variation in the weights.

For the proposed Sobolev loss approximations  $\mathcal{L}_{\text{strong},n}(u')$ ,  $\mathcal{L}_{\text{strong},n}^{\text{var}}(u')$ ,  $\mathcal{L}_{\text{weak},n}^{\text{var}}(u')$  the gradients

simplify due to the identities:

$$\begin{aligned} \nabla_w(r_{\text{strong},n,k}(u)) &= 2R_{m,n}^T W_{m,n,k} \\ \nabla_w(r_{\text{strong},n,k}^{\text{var}}(u)) &= 2R_{m,n}^T U_{m,n,k} \\ \nabla_w(r_{\text{weak},n,k}^{\text{var}}(u)) &= 2(H_{m,n}^T + F_{m,n}^T)U_{m,n,k} \\ &\quad + 2(G_{m,n}^T)V_{m-1,n,k-1/2} \\ \nabla_w(s_{\text{strong},n}(u)) &= 2R_{m,n}^T W_{m-1,n} \\ \nabla_w(s_{\text{strong},n,k}^{\text{var}}(u)) &= 2R_{m,n}^T V_{m-1,n,k-1/2}, \end{aligned} \quad (24)$$

where  $W_{m,n,k}$ ,  $U_{m,n,k}$ ,  $V_{m-1,n,k-1/2}$  are Sobolev cubature matrices from Eq. (11),(16).

We further investigate the Sobolev cubature properties in comparison to A.D. based PINNs below.

## 5. Polynomial Differentiation vs Automatic Differentiation

One of the main features of using the Sobolev cubatures, compared to the MSE loss, is that we can replace the problem of computing the derivatives of the PINN-surrogate, by computing them directly in the cubature. Below we present the complexity analysis for both, the normal PINN with *Automatic Differentiation (A.D.)* and the SC-PINN with *Polynomial Differentiation (P.D.)*.

**Theorem 4.** For a given deep Neural Network  $\hat{u}_\theta : \Omega \rightarrow \mathbb{R}$ , with architecture  $\xi_{m,1}$  consisting of  $l$  hidden layers and  $q$  neurons per layer, the complexity per epoch for computing the  $k$ -th derivative ( $\partial_x^k \hat{u}_\theta$ ) in  $s \in \mathbb{N}$  training points is given by

- i)  $\mathcal{O}(2^{k-1} l s q^2)$  for a PINN resting on A.D., i.e. it scales exponentially with the order of the derivative.
- ii)  $\mathcal{O}(\max\{s^2, l s q^2\})$  for the SC-PINN using P.D.

*Proof.* For proving i) we use the fact that a single backward pass required for computing the derivatives, has the same complexity as a forward pass, which is  $\mathcal{O}(l s q^2)$  due to (Baydin et al., 2018a). thus, for computing the first derivative at  $s$  points we need  $\mathcal{O}(l s q^2)$  operations. Due to the chain rule, computation of the second order derivatives causes the size of the dependency graph of the A.D. to double. By recursion of this fact the factor  $2^{k-1}$  appears as claimed.

For proving ii) we recall that the SC-PINN computes the  $k$ -th derivative by applying the pre-computed differential matrix  $\mathbb{D}^k := \Pi_{l=1}^k \mathbb{D}$ . Hence, for each epoch the costs of a matrix vector multiplication  $\mathbb{D}^k \hat{u}_\theta$  apply at each cubature (Legendre) node  $p \in P_{m,n}$ , with  $s = |P_{m,n}|$ . The product has  $\mathcal{O}(s^2)$  complexity per epoch and the evaluation  $\hat{u}_\theta(p)$ ,  $\forall p \in P_{m,n}$  has  $\mathcal{O}(l s q^2)$  complexity, yielding the result.  $\square$

*Example 5.* We consider a NN with architecture  $\Xi_{1,1} = \{1, 50, 50, 50, 50, 1\}$  given by four hidden layers of length 50. For  $s = 200$  training points computation of a 4-th order derivative computed with A.D. has a theoretical computational cost of  $1.6 \cdot 10^7$  operations while P.D. requires  $2 \cdot 10^6$  operations. In fact, the predicted factor-10-speed-up is achieved for the experiment in Section 6.7.

In addition to the derivative computation complexity, the SC-PINN formulation exploits the approximation power of the Gauss-Legendre cubature, as it becomes observable in the numerical experiments, Section 6.

Here, we want to point out the following insight: We consider the  $m$ -dimensional integral  $I[f] := \int_{\Omega} f d\Omega$  of a  $k$ -times differentiable function once approximated by the Gauss-Legendre cubature of degree  $n$ ,  $I_n^g[f] := \sum_{\alpha \in A_{m,n}} f^2(p_{\alpha}) \omega_{\alpha}$  and once by the Monte Carlo approximation  $I_n^M[f] := \frac{1}{N} \sum_{i \in I} f^2(x_i)$ , with  $K \subset \mathbb{R}^m$  a set of points of size  $|K| = |A_{m,n}|$ . Due to (Trefethen, 2017a) the approximations rates scale as:

$$|I[f] - I_n^g[f]| = \mathcal{O}\left(\frac{1}{k(n-k)^k}\right),$$

$$|I[f] - I_n^M[f]| = \mathcal{O}\left(\frac{1}{\sqrt{K}}\right), \quad K = (n+1)^m.$$

Hence, for regular functions,  $k \gg m$ , achieving a similar accuracy with the SC-PINNs requires less points compared to applying PINNs with MSE-losses. The limitations of the Sobolev cubatures start as the dimension  $m \gg 1$  of the domain becomes too high and the complexity in Theorem 4, i) is dominated by the  $\mathcal{O}(s^2)$ ,  $s = (n+1)^m$  term. We continue the comparison empirically in the next section.

## 6. Numerical Experiments

We designed the following experiments for validating and demonstrating our theoretical findings. All experiments were executed on the NVIDIA V100 cluster at HZDR. Pre-computation of the Sobolev cubature matrices is realized in (Suraz Cardona, 2022) as a feature of the open source package (Hernandez Acosta et al., 2021), which is based on our recent work (Hecht et al., 2017; 2018; 2020; Hecht & Sbalzarini, 2018). For comparison we benchmark the following schemes:

- i) *Classic PINNs (PINN)* as proposed in (Raissi et al., 2019) resting on the strong  $L^2$ -MSE loss, Eq. (1).
- ii) *Inverse Dirichlet Balancing (ID-PINNs)* with the  $L^2$ -MSE loss (Maddu et al., 2021), as described in the introduction.
- iii) *Sobolev Cubature PINNs (SC-PINNs)* with the weak  $L^2$ -loss for all the experiments unless specified otherwise.

- iv) *Variational PINNs (VPINNs)* with the strong  $L^2$ -loss with and without domain decomposition, as introduced in Section 1.1.2. While VPINNs resulted in incommensurate training effort in 2D only 1D experiments were executed.

For a given ground truth function  $g : \Omega \rightarrow \mathbb{R}$  and a  $\hat{u}_{\theta}$  approximation we measure the  $l_1, l_{\infty}$ -errors  $\epsilon_1 := \|\mathbf{g} - \mathbf{u}\|_1$ ,  $\epsilon_{\infty} := \|\mathbf{g} - \mathbf{u}\|_{\infty}$  by sampling on equidistant grids of size  $N = 100^2$  in 2D. For (inverse) parameter inference problems we denote the parameter error with  $\epsilon_{\lambda} = |\lambda - \lambda_{gt}|$ .

All models are trained with the same number of training points regardless of their specification (random or Legendre grids).

### 6.1. Poisson Equation

We start by addressing the Poisson problem in dimension  $m = 2$

$$\begin{cases} -\Delta u(x) - f(x) = 0 & , \forall x \in \Omega = [-1, 1]^2 \\ u(x) - g(x) = 0 & , \forall x \in \partial\Omega, \end{cases}$$

described in detail Eq. (13). We choose  $f(x, y) := -2\lambda^2 \cos(\lambda x) \sin(\lambda y)$  and  $g(x) := \cos(\lambda x) \sin(\lambda y)$ , with frequency  $\lambda = 2\pi q$ ,  $q = 6$ , yielding  $u(x, y) = g(x, y)$  to be the analytic solution.

We compare the performance of the following PINN implementations:

- I) PINN and ID-PINN relying in strong *mean square* (MSE) loss  $\mathcal{L}_{\text{MSE}}$ , Eq. (1).
- II) SC-PINN with strong Sobolev loss  $\mathcal{L}_{\text{strong}}$ , Eq. (17),

$$\mathcal{L}_{\text{strong}}(u) = r_{\text{strong}, n_r, k}(u) + s_{\text{strong}, n_s, l}(u)$$

for  $k = 0, l = 2, n_r = 30, n_s = 100$ , in two versions: Once computing  $\Delta u$  with automatic differentiation (A.D.) and once without A.D., but with *polynomial differentiation* (P.D.) given in Eq. (20).

- III) SC-PINN with strong variational Sobolev loss, Eq. (22)  $\mathcal{L}_{\text{strong}}^{\text{var}}$

$$\mathcal{L}_{\text{strong}}^{\text{var}}(u) = r_{\text{strong}, n_r, k}^{\text{var}}(u) + s_{\text{strong}, n_s, l}^{\text{var}}(u)$$

for  $k = 0, l = 0, n_r = 30, n_s = 100$ , without A.D., but with P.D..

All methods were implemented for fully connected feed-forward NNs,  $\hat{u} \in \Xi_{2,1}$ , of 5 hidden layers, each of 50 units length, unless specified otherwise. Activation functions were chosen as  $\sigma(x) = \sin(x)$ , which performed best compared to trials with ReLU, ELU or  $\sigma(x) = \tanh(x)$ .

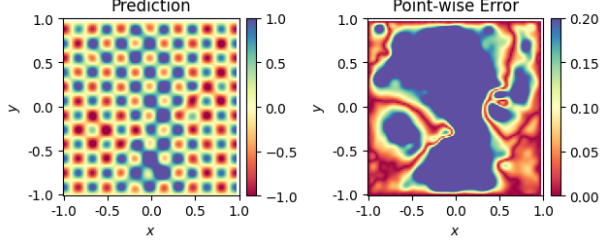


Figure 1. ID-PINN with MSE loss, reaching  $\epsilon_\infty = 1.24$ ,  $\epsilon_1 = 2.22\text{e-}1$ ,  $t \approx 1173$ .

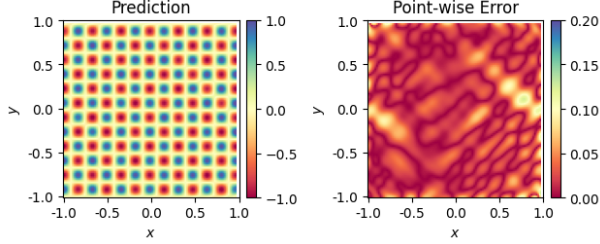


Figure 2. SC-PINN with strong Sobolev loss and A.D., reaching  $\epsilon_\infty = 1.37\text{e-}1$ ,  $\epsilon_1 = 2.27\text{e-}2$ ,  $t \approx 725$ .

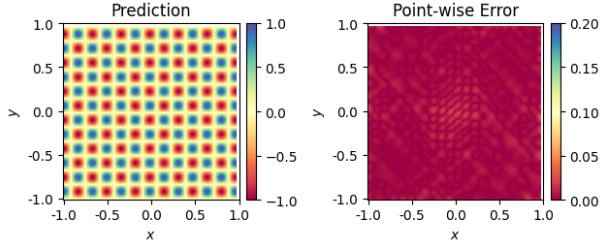


Figure 3. SC-PINN with strong Sobolev loss and P.D., reaching  $\epsilon_\infty = 3.00\text{e-}2$ ,  $\epsilon_1 = 3.75\text{e-}3$ ,  $t \approx 192$ .

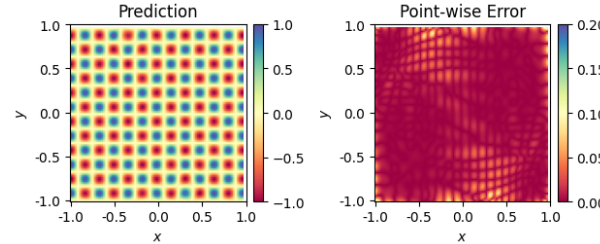


Figure 4. SC-PINN with strong variational Sobolev loss and P.D., reaching  $\epsilon_\infty = 1.25\text{e-}1$ ,  $\epsilon_1 = 7.70\text{e-}3$ ,  $t \approx 188$ .

All PINNs were trained by applying the Adam optimizer (Kingma & Ba, 2014) for 30000 iterations, batch size  $bs = |P_{m,n}|$  for ID-PINN equals SC-PINN, and learning rate of  $lr = 1\text{e-}3$ , whereas ID-PINN applies its dynamic gradient balancing scheme.

Approximation errors and CPU-training times  $t$  are reported in Figs. 1–4. While the classic PINN approach failed to converge (reach reasonable approximations) its results are

skipped.

In comparison SC-PINN reaches several orders of magnitude better approximations: SC-PINN with  $\mathcal{L}_{\text{strong}}$  and A.D. improves by one order, while replacing A.D. with P.D. even increases the accuracy by one further order. In addition the CPU runtime is reduced by three fold when executing SC-PINN with P.D. instead of A.D. The choice of  $\mathcal{L}_{\text{strong}}^{\text{var}}$  improves the  $\epsilon_1$  error by one order of magnitude compared to SC-PINN with  $\mathcal{L}_{\text{strong}}$  and A.D., which requires more CPU time.

We address a further prominent PDE problems to continue our empirical investigations. From here on we only use P.D. instead of A.D. for executing the experiments with the SC-PINNs.

## 6.2. Quantum Harmonic Oscillator

The time independent *Quantum Harmonic Oscillator* in dimension  $m = 2$ , corresponds to the *Schrödinger equation* with the linear potential  $V(u(x)) := (x_1^2 + x_2^2)u(x)$ ,  $u \in C^2(\Omega, \mathbb{R})$ , see e.g. (Liboff, 1980; Griffiths & Schroeter, 2018), given by:

$$\begin{cases} -\Delta u(x) + V(u(x)) &= \lambda u(x) \quad , \forall x \in \Omega \\ u(x) - g(x) &= 0 \quad , \forall x \in \partial\Omega, \end{cases}$$

We consider the eigenvalue problem  $\lambda = n_1 + n_2 + 1$ ,  $n_1, n_2 \in \mathbb{N}$  with eigenfunctions

$$g(x_1, x_2) = \frac{\pi^{-1/4}}{\sqrt{2^{n_1+n_2} n_1! n_2!}} e^{-\frac{(x_1^2 + x_2^2)}{2}} H_{n_1}(x_1) H_{n_2}(x_2),$$

whereas  $H_n$  denotes the  $n$ -th *Hermite polynomial*.

We keep the experimental design from Section 6.1, choose  $\lambda = 15$  and report the results in Fig. 5–7: Similar to the previous experiment classic PINN failed to converge, SC-PINNs improve the accuracy up to 2 orders of magnitude in 4 fold less runtime, whereas, SC-PINN with  $\mathcal{L}_{\text{strong}}^{\text{var}}$  and P.D. performs best.

## 6.3. Poisson problems with hard transitions

We re-investigate PINN-solutions of the Poisson problem in dimension  $m = 1$ , whose analytic solutions include hard transitions. That is, choosing

$$f(x) := C(A\omega^2 \sin(\omega x) + 2\beta^2 \text{sech}^2(x) \tanh(\beta x)),$$

with boundary condition  $g(x) := C(A \sin(\omega x) + \tanh(\beta x))$  yielding  $u(x) = g(x)$  to be the analytic solution. Two scenarios were considered:

$$S_1 = \{C = 0.1, A = 0.1, \beta = 30, \omega = 20\pi, bs = 100\}$$

$$S_2 = \{C = 0.1, A = 0.1, \beta = 5, \omega = 26.5\pi, bs = 100\}$$

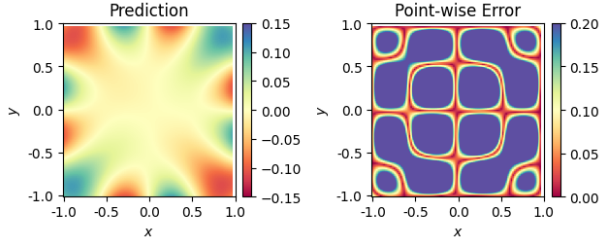


Figure 5. ID-PINN with MSE loss and A.D., reaching  $\epsilon_\infty = 1.46\text{e-}1$ ,  $\epsilon_1 = 4.78\text{e-}2$ ,  $t \approx 905$ ,

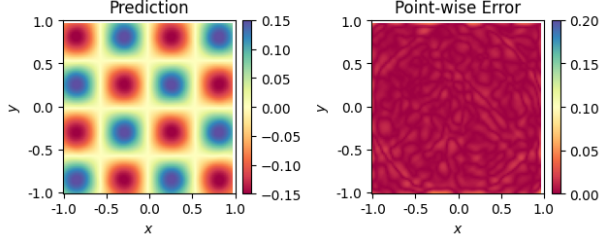


Figure 6. SC-PINN with strong Sobolev loss and P.D., reaching,  $\epsilon_\infty = 1.22\text{e-}2$ ,  $\epsilon_1 = 1.24\text{e-}3$ ,  $t \approx 165$ ,

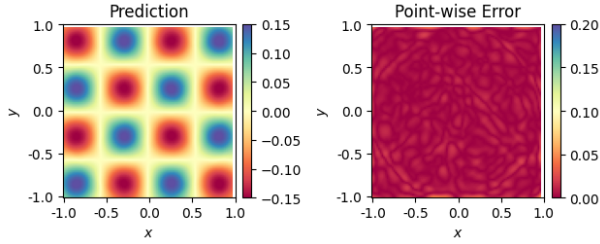


Figure 7. SC-PINN with strong variational Sobolev loss and P.D., reaching,  $\epsilon_\infty = 7.27\text{e-}3$ ,  $\epsilon_1 = 8.16\text{e-}4$ ,  $t \approx 167$ ,

Up to reducing to 4 hidden layers, each of 20 units length the same NN architecture,  $\hat{u} \in \Xi_{1,1}$ , as prior was chosen. The degree  $n \in \mathbb{N}$  of the Sobolev losses is set as the batch size  $n = \text{bs}$ . In addition to the previous PINN methods we consider the VPINNs, introduced in Section 1.1.2, relying on the strong variational Sobolev loss and domain decomposition specified by the number of its elements  $N_{\text{el}} \in \mathbb{N}$ .

Comparison of SC-PINNs and VPINNs for scenario  $S_1$  is reported in Figs. 8,9: While SC-PINN with strong Sobolev loss misses to capture the solution, SC-PINN with variational loss reaches compatible approximations compared to VPINN with 3-element decomposition  $N_{\text{el}} = 3$ .

For the second set of parameters  $S_2$  results are reported in Fig. 10: We observe a similar behaviour as in scenario  $S_1$ , but SC-PINN with strong variational loss reaches one order of magnitude better (overall)  $\epsilon_1$ -error compared to VPINN. ID-PINN and PINN both fail to converge. We

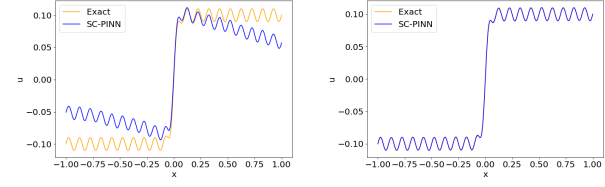


Figure 8. SC-PINN with strong Sobolev loss and P.D. (left), reaching  $\epsilon_\infty = 3.04\text{e-}2$ ,  $\epsilon_1 = 7.24\text{e-}2$ ,  $t \approx 150$ , SC-PINN with strong variational Sobolev loss and P.D.(right), reaching  $\epsilon_\infty = 2.0\text{e-}3$ ,  $\epsilon_1 = 4.0\text{e-}4$ ,  $t \approx 151$ , scenario  $S_1$ .

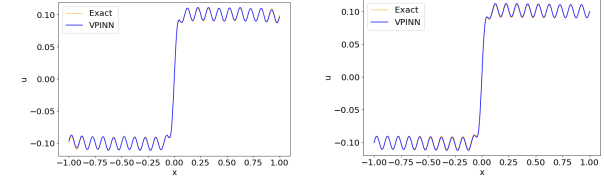


Figure 9. VPINN with  $N_{\text{el}} = 1$  (left), reaching  $\epsilon_\infty = 3.29\text{e-}3$ ,  $\epsilon_1 = 9.94\text{e-}4$ ,  $t \approx 96$ , VPINN with  $N_{\text{el}} = 3$  (right), reaching  $\epsilon_\infty = 2.73\text{e-}3$ ,  $\epsilon_1 = 1.40\text{e-}3$ ,  $t \approx 191$ , scenario  $S_1$ .

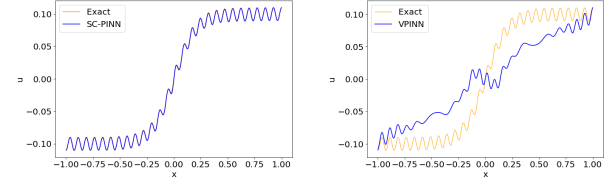


Figure 10. SC-PINN with strong variational Sobolev loss and P.D.(left), reaching  $\epsilon_\infty = 2.75\text{e-}3$ ,  $\epsilon_1 = 5.35\text{e-}4$ ,  $t \approx 151$ , VPINN with  $N_{\text{el}} = 3$ , reaching  $\epsilon_\infty = 6.50\text{e-}2$ ,  $\epsilon_1 = 3.40\text{e-}2$ , scenario  $S_2$ ,  $t \approx 180$ .

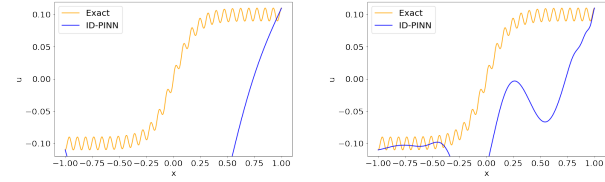


Figure 11. ID-PINN with MSE loss,  $\text{bs} = 500$  and A.D.,(left), reaching  $\epsilon_\infty = 4.74\text{e-}1$ ,  $\epsilon_1 = 2.50\text{e-}1$ ,  $t \approx 158$ , ID-PINN with MSE loss without I.D.,  $\text{bs} = 5000$  and A.D.,(right), reaching  $\epsilon_\infty = 1.73\text{e-}1$ ,  $\epsilon_1 = 7.13\text{e-}2$ ,  $t \approx 360$ , scenario  $S_2$ .

present the results only for the I.D. balancing, once for batch size  $\text{bs} = 500$  and once for  $\text{bs} = 5000$ , are reported in Fig. 11. We, however, observe that even by increasing the batch size by a factor of 10 ID-PINN does not become compatible to SC-PINN.



#### 6.4. 2D Poisson Inverse Problem

We will now consider the inverse problem for the 2D Poisson equation, where we want to infer  $\lambda$ , that appears explicitly on the RHS  $f(x) = \lambda \cos(\omega x) \sin(\omega y)$  for  $\omega = \pi$ . We used for the SC-PINN, degree 100 and 30 quadrature for the boundary and the domain respectively and the same amount of points randomly sampled for the ID-PINN and the standard PINN. The ground truth  $\lambda_{gt} = 2\omega^2$  and the weak  $L^2$ -loss. We test it against the standard PINN and the ID-PINN with same number of points.

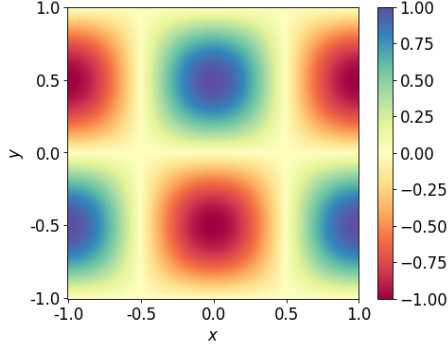


Figure 12. Solution for 2D Poisson with  $\lambda_{gt} = \pi$ .

Method	Approximation error		Runtime (s)
	$\epsilon_\lambda$	$\epsilon_1$	
PINN	$4.63 \cdot 10^{-1}$	$1.13 \cdot 10^{-2}$	$t \approx 1592$
ID-PINN	$2.14 \cdot 10^{-2}$	$8.09 \cdot 10^{-4}$	$t \approx 2184$
SC-PINN	<b><math>3 \cdot 10^{-4}</math></b>	<b><math>5.49 \cdot 10^{-4}</math></b>	<b><math>t \approx 103</math></b>

Table 1. Errors for 2D Poisson inverse problem

Due to Table 1, the SC-PINN recovers the parameter  $\lambda$  with one order of magnitude higher accuracy by requiring almost two orders of magnitude less runtime. even in the inverse problem setting, this shows the superiority of SC-PINN in both approximation and computational performance. To support this result, we consider the inverse problem for the time independent 2D QHO.

#### 6.5. 2D QHO Inverse Problem

We pose the QHO eigenvalue problem for unknown eigenvalue  $\lambda_{gt} = 5$  and seek finding the eigenvalue and the PDE solution simultaneously. In this setting we use the SC-PINN with  $L^2$ -weak loss, and a 200 degree cubature for the boundary and use degree 50 in the domain. We compare it with the ID-PINN and the standard PINN trained with the same number of (random) training points.

Table 2 shows that SC-PINN outperforms the ID-PINN and the PINN by inferring  $\lambda$  with four orders of magnitude better accuracy and recovers the PDE solution with one order of magnitude higher precision. On top, SC-PINN requires two

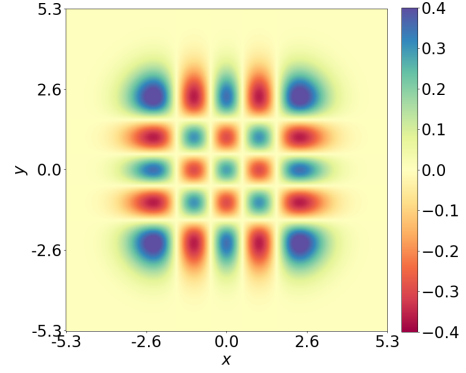


Figure 13. Solution for 2D QHO with  $\lambda_{gt} = 5$ .

Method	Approximation error		Runtime (s)
	$\epsilon_\lambda$	$\epsilon_1$	
PINN	6.01	$7.32 \cdot 10^{-2}$	$t \approx 1414$
ID-PINN	$6.21 \cdot 10^{-2}$	$7.51 \cdot 10^{-3}$	$t \approx 1346$
SC-PINN	<b><math>2.18 \cdot 10^{-4}</math></b>	<b><math>5.68 \cdot 10^{-4}</math></b>	<b><math>t \approx 192</math></b>

Table 2. Errors for 2D QHO inverse problem with  $\lambda_{gt} = 5$

orders of magnitude less runtime. This demonstrates once more the superiority of the method SC-PINN when applied to forward and inverse problems.

#### 6.6. Non-linear Burger's Equation in 1D

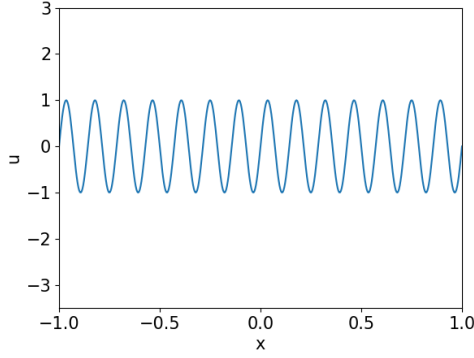
We consider the time independent Burger's equation in conservative form with Dirichlet boundary conditions given by

$$\begin{cases} -\frac{d^2}{dx^2}u(x) + \frac{1}{2}\frac{d}{dx}(u(x)^2) = f(x) & , \forall x \in \Omega \\ u(x) - g(x) = 0 & , \forall x \in \partial\Omega, \end{cases}$$

with  $f(x) := \frac{\omega}{2}\sin(2\omega x) + \omega^2\sin(\omega x)$ .

We solve the PDE with a 100 degree quadrature,  $\omega = 14\pi$  and the and strong variational loss for the SC-PINN norm. We test it against the PINN and the ID-PINN with same number of (random) training points.

According to the results presented in Table 3 SC-PINN performs again better than the other PINN formulations by reaching 2 orders of magnitude smaller  $\epsilon_1$ -error. However, SC-PINN is slightly slower than the other PINNs in this 1D-setting. We focus on the runtime performance in a separate experiment below.


 Figure 14. Solution for 1D Burger's with  $\omega = 14\pi$ .

Method	Approximation error		Runtime (s)
	$\epsilon_1$	$\epsilon_\infty$	
PINN	$2.2 \cdot 10^{-1}$	$4.2 \cdot 10^{-1}$	$t \approx 125$
ID-PINN	$7.9 \cdot 10^{-1}$	2.6	$t \approx 138$
SC-PINN	$2.7 \cdot 10^{-3}$	$8.7 \cdot 10^{-3}$	$t \approx 157$

Table 3. Errors for 1D Burger's forward problem

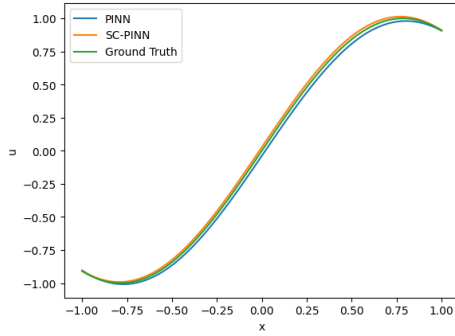


Figure 15. Solution of 4-th order ODE

Method	Approximation error		Runtime (s)
	$\epsilon_\lambda$	$\epsilon_1$	
PINN	$2.52 \cdot 10^{-1}$	$3.93 \cdot 10^{-2}$	$t \approx 278.7$
SC-PINN	$1.4 \cdot 10^{-2}$	$2.8 \cdot 10^{-2}$	$t \approx 25.72$

Table 4. Errors for the 4th order ODE

### 6.7. Polynomial Differentiation vs Automatic Differentiation

We consider the forward problem of the following 4th order ODE:

$$\frac{d^4}{dx^4}y = f(x), \forall x \in \Omega,$$

where  $f(x) := -\omega^4 \sin(\omega x)$  with  $y(0) = \sin(\omega 0)$ . We benchmark the SC-PINN with P.D. against the standard PINN with MSE loss,  $bs = 101$  training points, 10000 epochs executed by the Adam optimizer (Kingma & Ba, 2014).

As reported in Table 4 the SC-PINN recovers a more accurate solution of the 4th order ODE in one order of magnitude less runtime. This suggests that replacing A.D. by P.D. increases the efficiency, as predicted in our discussions in Section 5, Example 5.

## 7. Conclusion

We introduced the notion of Sobolev cubatures and gave theoretical insights in order to setup the novel Sobolev PINNs (SC-PINNs). As predicted, by the runtime complexity analysis we did, for low dimensional problems this results in a faster PDE learning scheme than PINNs relying on automatic differentiation.

Moreover, in Theorem 3 we theoretically ensured that the SC-PINNs converge to strong (smooth) PDE solutions for well posed problems. This result is complemented by the several order of magnitude higher accuracy the SC-PINNs reached when considering prominent linear, non-linear, forward, and inverse PDE problems.

Depending on the numerical experiment, the choice of the Sobolev cubature differed. While we meanwhile deepened the theoretical insights presented in this article to deliver the optimal choice beforehand these subjects are out of scope, here, and part of a follow-up study. This includes a relaxation of the Sobolev cubatures, resisting the curse of dimensionality when addressing higher dimensional problems.

Apart from these potential enhancements the class of low dimensional,  $\dim = 2, 3, 4$ , real world problems is huge. Thus, the demonstrations, here, make us believe that applying the SC-PINNs might be beneficial for many scientific applications across all disciplines.

## 8. Acknowledgements

We would like to thank Dominik Sturm from the Center for Advanced Systems Understanding, for the useful discussions and support during the whole project, as well as for providing the base framework for training the PINNs and the ID-PINNs.

## References

- Adams, R. A. and Fournier, J. J. *Sobolev spaces*, volume 140. Academic press, 2003.
- Anthony, M. and Bartlett, P. L. *Neural network learning: Theoretical foundations*. Cambridge University press, 2009.
- Arjovsky, M., Chintala, S., and Bottou, L. Wasserstein generative adversarial networks. In Precup, D. and Teh,

- Y. W. (eds.), *Proceedings of the 34th International Conference on Machine Learning*, volume 70 of *Proceedings of Machine Learning Research*, pp. 214–223. PMLR, 06–11 Aug 2017. URL <https://proceedings.mlr.press/v70/arjovsky17a.html>.
- Baydin, A. G., Pearlmutter, B. A., Radul, A. A., and Siskind, J. M. Automatic differentiation in machine learning: a survey. *Journal of Machine Learning Research*, 18(153): 1–43, 2018a. URL <http://jmlr.org/papers/v18/17-468.html>.
- Baydin, A. G., Pearlmutter, B. A., Radul, A. A., and Siskind, J. M. Automatic differentiation in machine learning: a survey. *Journal of machine learning research*, 18, 2018b.
- Bernardi, C. and Maday, Y. Spectral methods. *Handbook of numerical analysis*, 5:209–485, 1997.
- Brezis, H. *Functional analysis, Sobolev spaces and partial differential equations*, volume 2. Springer, 2011.
- Canuto, C., Hussaini, M. Y., Quarteroni, A., and Zang, T. A. *Spectral methods: fundamentals in single domains*. Springer Science & Business Media, 2007.
- De Branges, L. The Stone-Weierstrass Theorem. *Proceedings of the American Mathematical Society*, 10(5): 822–824, 1959.
- Ern, A. and Guermond, J.-L. *Theory and practice of finite elements*, volume 159. Springer, 2004.
- Goodfellow, I., Bengio, Y., and Courville, A. *Deep learning*. MIT press, 2016.
- Griffiths, D. J. and Schroeter, D. F. *Introduction to quantum mechanics*. Cambridge University Press, 2018.
- Hecht, M. and Sbalzarini, I. F. Fast interpolation and Fourier transform in high-dimensional spaces. In Arai, K., Kapoor, S., and Bhatia, R. (eds.), *Intelligent Computing. Proc. 2018 IEEE Computing Conf., Vol. 2.*, volume 857 of *Advances in Intelligent Systems and Computing*, pp. 53–75, London, UK, 2018. Springer Nature.
- Hecht, M., Cheeseman, B. L., Hoffmann, K. B., and Sbalzarini, I. F. A quadratic-time algorithm for general multivariate polynomial interpolation. *arXiv preprint arXiv:1710.10846*, 2017.
- Hecht, M., Hoffmann, K. B., Cheeseman, B. L., and Sbalzarini, I. F. Multivariate Newton interpolation. *arXiv preprint arXiv:1812.04256*, 2018.
- Hecht, M., Gonciarz, K., Michelfeit, J., Sivkin, V., and Sbalzarini, I. F. Multivariate interpolation in unisolvent nodes—lifting the curse of dimensionality. *arXiv preprint arXiv:2010.10824*, 2020.
- Hernandez Acosta, U., Krishnan Thekke Veettil, S., Wicaksono, D., and Hecht, M. MINTERPY - multivariate interpolation in python. <https://github.com/casus/minterpy/>, 2021.
- Jost, J. *Partial Differential Equations*. New York: Springer-Verlag, 2002.
- Kharazmi, E., Zhang, Z., and Karniadakis, G. E. Variational physics-informed neural networks for solving partial differential equations. *arXiv preprint arXiv:1912.00873*, 2019.
- Kharazmi, E., Zhang, Z., and Karniadakis, G. E. hp-vpinns: Variational physics-informed neural networks with domain decomposition. *ArXiv*, abs/2003.05385, 2020.
- Kingma, D. P. and Ba, J. Adam: A method for stochastic optimization. *arXiv preprint arXiv:1412.6980*, 2014.
- LeVeque, R. J. *Finite difference methods for ordinary and partial differential equations: steady-state and time-dependent problems*. SIAM, 2007.
- Li, S. and Liu, W. K. *Meshfree particle methods*. Springer Science & Business Media, 2007.
- Liboff, R. L. *Introductory Quantum Mechanics*. Addison-Wesley Publishing Company. Canadá, 1980.
- Long, Z., Lu, Y., Ma, X., and Dong, B. Pde-net: Learning pdes from data. *ArXiv*, abs/1710.09668, 2018.
- Maddu, S., Sturm, D., Müller, C. L., and Sbalzarini, I. F. Inverse dirichlet weighting enables reliable training of physics informed neural networks. *Machine Learning: Science and Technology*, 2021. URL <http://iopscience.iop.org/article/10.1088/2632-2153/ac3712>.
- Raissi, M., Perdikaris, P., and Karniadakis, G. Physics-informed neural networks: A deep learning framework for solving forward and inverse problems involving nonlinear partial differential equations. *Journal of Computational Physics*, 378:686–707, 2019. ISSN 0021-9991. doi: <https://doi.org/10.1016/j.jcp.2018.10.045>. URL <https://www.sciencedirect.com/science/article/pii/S0021999118307125>.
- Sirignano, J. A. and Spiliopoulos, K. Dgm: A deep learning algorithm for solving partial differential equations. *Journal of Computational Physics*, 2018.
- Stroud, A. *Approximate calculation of multiple integrals: Prentice-Hall series in automatic computation*. Prentice-Hall (Englewood Cliffs, NJ), 1971.
- Stroud, A. Secrest, d.(1966). Gaussian quadrature formulas, 2011.

- Suraz Cardona, J. E. Sobolev cubature based PDE-learning. [https://github.com/casus/PDE\\_learning/](https://github.com/casus/PDE_learning/), 2022.
- Trefethen, L. N. Cubature, approximation, and isotropy in the hypercube. *SIAM Review*, 59(3):469–491, 2017a.
- Trefethen, L. N. Multivariate polynomial approximation in the hypercube. *Proceedings of the American Mathematical Society*, 145(11):4837–4844, 2017b.
- Trefethen, L. N. *Approximation theory and approximation practice*, volume 164. SIAM, 2019.
- Wang, S., Teng, Y., and Perdikaris, P. Understanding and mitigating gradient flow pathologies in physics-informed neural networks. *SIAM Journal on Scientific Computing*, 43(5):A3055–A3081, 2021.
- Weierstrass, K. Über die analytische Darstellbarkeit sogenannter willkürlicher Funktionen einer reellen Veränderlichen. *Sitzungsberichte der Königlich Preussischen Akademie der Wissenschaften zu Berlin*, 2:633–639, 1885.
- Yang, L., Zhang, D., and Karniadakis, G. E. Physics-informed generative adversarial networks for stochastic differential equations. *ArXiv*, abs/1811.02033, 2020.